# NBS1 Knockdown by Small Interfering RNA Increases Ionizing Radiation Mutagenesis and Telomere Association in Human Cells

Ying Zhang,[1] Chang U.K. Lim,[1] Eli S. Williams,[1] Junqing Zhou,[1] Qinming Zhang,[1] Michael H. Fox,[1] Susan M. Bailey,[1,2] and Howard L. Liber[1,2]

[1]Department of Environmental and Radiological Health Sciences, Colorado State University, Fort Collins, Colorado and
[2]University of Colorado Cancer Center, Denver, Colorado

## Abstract

Hypomorphic mutations which lead to decreased function of the NBS1 gene are responsible for Nijmegen breakage syndrome, a rare autosomal recessive hereditary disorder that imparts an increased predisposition to development of malignancy. The NBS1 protein is a component of the MRE11/RAD50/NBS1 complex that plays a critical role in cellular responses to DNA damage and the maintenance of chromosomal integrity. Using small interfering RNA transfection, we have knocked down NBS1 protein levels and analyzed relevant phenotypes in two closely related human lymphoblastoid cell lines with different p53 status, namely wild-type TK6 and mutated WTK1. Both TK6 and WTK1 cells showed an increased level of ionizing radiation–induced mutation at the TK and HPRT loci, impaired phosphorylation of H2AX ($\gamma$-H2AX), and impaired activation of the cell cycle checkpoint regulating kinase, Chk2. In TK6 cells, ionizing radiation–induced accumulation of p53/p21 and apoptosis were reduced. There was a differential response to ionizing radiation–induced cell killing between TK6 and WTK1 cells after NBS1 knockdown; TK6 cells were more resistant to killing, whereas WTK1 cells were more sensitive. NBS1 deficiency also resulted in a significant increase in telomere association that was independent of radiation exposure and p53 status. Our results provide the first experimental evidence that NBS1 deficiency in human cells leads to hypermutability and telomere associations, phenotypes that may contribute to the cancer predisposition seen among patients with this disease. (Cancer Res 2005; 65(13): 5544-53)

## Introduction

Mutation of the NBS1 gene is responsible for the chromosomal breakage disorder, Nijmegen breakage syndrome, a rare autosomal recessive hereditary disorder characterized by increased predisposition to development of malignancy at an early age, especially lymphomas and leukemias (1–3). Cells isolated from Nijmegen breakage syndrome patients exhibit cellular phenotypic alterations, very similar to those seen in ataxia telangiectasia, including hypersensitivity to ionizing radiation, chromosome fragility (4), and abnormal cell cycle checkpoint regulation (5, 6).

The NBS1 gene contains 16 exons encompassing about 49,000 bp of genomic sequence on chromosome 8q21 (7, 8). The NBS1 protein, a component of the MRE11/RAD50/NBS1 (MRN) complex, plays an important role in DNA double-strand break repair by homologous recombination, nonhomologous end-joining, meiotic recombination, and telomere maintenance (4, 5). The FHA/BRCT domain in the NH$_2$-terminal region of NBS1 protein directly binds to phosphorylated H2AX ($\gamma$-H2AX), then recruits the other members of the complex to the sites of DNA double-strand breaks (9). The COOH-terminal region of the NBS1 protein binds MRE11/RAD50 (10–13). Several serine/glutamine motifs, consensus sequences of phosphorylation by ataxia telangiectasia mutated (ATM) and ATM/RAD3-related, are found at the central region of NBS1. In particular, the serine residues at 278 and 343 are phosphorylated by ATM kinase in response to ionizing radiation both in vitro and in vivo, and such phosphorylation is responsible for intra-S phase checkpoint control (14, 15) and telomere maintenance (11, 13, 16). Recently, it was shown that the MRN complex is required for ATM activation after treatment with DNA double-strand break–inducing agents, suggesting roles for the MRN complex both upstream and downstream of ATM in the DNA damage response pathway (17, 18).

The NBS1 protein has been implicated in multiple cellular responses related to DNA damage, including cell cycle control, DNA replication and repair, and the maintenance of chromosomal stability. Therefore, alterations in any of these processes could be related to increased mutation rates of cancer-related genes, ultimately contributing to carcinogenesis. Certainly, there is indirect evidence to support this view, including retrospective observations that Nijmegen breakage syndrome patients have an increased cancer predisposition and cells derived from Nijmegen breakage syndrome patients exhibit increased chromosomal aberrations (2, 19). Consistent with this, mice heterozygous for NBN (the murine homologue of NBS1) developed a wide variety of tumors affecting the liver, mammary gland, prostate, and lung, in addition to lymphomas. Moreover, cytogenetic analysis revealed that primary NBN$^{+/-}$ embryonic fibroblasts and tumor cells exhibited increased levels of chromosomal aberrations (20). Although presumably NBS1 deficiency might play an important role in the process of gene mutation, no direct experimental evidence is available.

An S phase–specific association of NBS1 with the telomeric binding protein TRF2 has also been shown (11), implicating the MRN complex in normal telomere maintenance and integrity. In support of this, telomere shortening and instability was recently shown in a human tumor cell line expressing an NBS1 allele with mutated ATM-phosphorylation sites (16). Telomere associations are cytogenetic anomalies in which telomeres are observed in unusually close proximity to one another; these events have been reported not only in ataxia telangiectasia (21, 22), but also in tumor

---

Requests for reprints: Ying Zhang, Department of Environmental and Radiological Health Sciences, Colorado State University, Fort Collins, CO 80523. Phone: 970-491-0574; Fax: 970-491-0623; E-mail: Ying.Zhang@colostate.edu.

cells, for example, from breast cancer (23). The cause of telomere association and their downstream effects are not well understood. Here, we report the involvement of the NBS1 protein in normally preventing or reducing these telomere association events.

Small interfering RNA (siRNA) posttranscriptional targeted gene silencing is a powerful technique that enhances study of the biological function of specific genes. This approach introduces a transient decrease in protein expression of the targeted gene (24). It can provide an advantage over traditional gene knock-out, especially when considering disruption of a critical gene that may be functionally important for the maintenance of genomic integrity, because permanent absence of the protein may make subsequent analysis impossible. Indeed, gene knock-out of *NBS1* results in embryonic lethality at the blastocyst stage due to growth retardation and increased apoptosis (20), thus preventing further study of its role in the process of mutagenesis and carcinogenesis. Here, we report the consequences of the transient knockdown of NBS1 protein by siRNA in human cells on ionizing radiation– induced Chk2 and p53 activation, γ-H2AX levels, telomere instability, cell killing, and mutation. Knockdowns are of particular relevance to diseases like Nijmegen breakage syndrome, which exhibit a hypomorphic phenotype.

## Materials and Methods

**Cell culture and γ-irradiation.** The human B-lymphoblast cell lines, TK6 and WTK1, were derived from the same progenitor, WIL2 (25, 26). TK6 and WTK1 were maintained in RPMI 1640 supplemented with 10% horse serum, 100 units/mL penicillin, and 100 μg/mL streptomycin. γ-Irradiations were done at room temperature in a calibrated Mark I $^{137}$Cs γ-irradiator (J.L. Shepherd and Associates, Glendale, CA). Log-phase cells were irradiated at $1 \times 10^6$ per mL in 10 mL of growth medium in T-25 flasks with doses of 0.75 to 3 Gy. Dose rates ranged from 0.20 to 0.25 Gy/minute.

**Small interfering RNA transfection.** The siRNA sequence (leading strand) used for *NBS1* gene silencing was: r(GGCGUGUCAGUUGAU-GAAA)d(TT). Transfections were done according to the instructions of the supplier (Qiagen, Valencia, CA), in serum-free RPMI 1640 at a density of $8 \times 10^5$ cells/mL. The concentration of siRNAs was 20 nmol/L in transfections, which were prepared in the form of siRNA/Lipofect-AMINE2000 (Invitrogen, Carlsbad, CA) complexes (1:1.5). Horse serum was added to 10% 6 hours later. Cell samples were collected daily for immunoblotting and immunofluorescence assays.

**Immunoblotting and immunofluorescence assay.** Cells ($6 \times 10^6$) were lysed in 200 μL ice-cold lysis buffer [50 mmol/L Tris-HCl (pH 7.4), 150 mmol/L NaCl, 0.5% sodium deoxycholate, 0.1% SDS, 1% Triton X-100, 5 mmol/L EDTA (pH 8.0)] containing protease inhibitors (1 mmol/L phenylmethylsulfonyl fluoride, 0.1% aprotinin, 0.1% leupeptin, 1 mmol/L sodium orthovanadate, 1 mmol/L sodium fluoride). Protein concentrations of the lysates were determined using the bicinchoninic acid protein assay kit (Pierce, Rockford, IL). Cell lysates were loaded and electrophoresed on 10% SDS polyacrylamide gels. After wet-blotting to nitrocellulose, protein level was analyzed using the corresponding primary mouse monoclonal antibodies NBS1, p53, p21, β-actin (Abcam, Cambridge, MA) and Chk2-Thr[68] (Cell Signaling Technology, Beverly, MA), then horseradish peroxi-dase–conjugated goat anti-mouse IgG (Abcam). The immunoreactive bands were visualized by chemiluminescence on X-ray films. Protein levels were quantified by using ImageQuant V5.1 software (Molecular Dynamics, Piscataway, NJ) and corrected with a loading control. For the immunofluorescence assay, cells were centrifuged onto slides and then fixed with 4% paraformaldehyde at 4°C for 10 minutes. After permeabilization with 0.2% Triton X-100 in PBS for 5 minutes, cells were incubated with NBS1 antibody and then FITC-conjugated goat anti-mouse IgG. Slides were examined by fluorescence microscopy.

**Apoptosis sub-G$_1$ assay.** The sub-G$_1$ method for measuring apoptosis relies on the loss of cleaved DNA (low molecular weight DNA) from the nucleus resulting in a smaller amount of DNA in the cell. After staining the cells with a DNA stain such as propidium iodide and analyzing them by flow cytometry, a subdiploid peak is obtained, representing apoptotic cells which have lost some of their DNA (27). Cells were fixed in ice-cold 70% ethanol, centrifuged, and washed once with PBS, then resuspended in 1 mL permeabilization buffer [192 parts of 0.2 mol/L Na$_2$HPO$_4$ and 8 parts of 0.1 mol/L sodium citrate (pH 7.8)] for 35 minutes at room temperature. The cells were resuspended in 1 mL PBS containing 25 μg/mL propidium iodide and 40 Kunitz units RNase A (Sigma, St. Louis, MO) for at least 20 minutes. The stained cells were filtered and analyzed by flow cytometry.

**γ-H2AX labeling assay.** Cells were first fixed in 1% paraformaldehyde solution at 4°C for 15 minutes, then fixed in ice-cold 80% ethanol and resuspended in permeabilization buffer (0.25% Triton X-100 in PBS) for 30 minutes on ice. The cells were resuspended in mouse monoclonal anti γ-H2AX antibody (Upstate Biotechnology, Lake Placid, NY) with 1:250 dilution in TBFP (0.5% Tween 20, 1% bovine serum albumin, and 1% fetal bovine serum in PBS) and incubated for 2 hours at room temperature. Cells were then incubated for 30 minutes on ice in 100 μL Alexa Fluor 488 F(ab′)2 fragment of goat anti-mouse IgG (heavy and light chains, H&L; 2 mg/mL; Molecular Probes, Eugene, OR) with 1:200 dilution in TBFP. The stained cells were filtered and analyzed by flow cytometry.

**Flow cytometry analysis.** All cell samples were analyzed with a CyAnLX flow cytometer interfaced to Summit software (DakoCytomation, Carpinteria, CA). Excitation with a (20 mmol/L) 488 nm sapphire solid state laser Alexa Fluor. Fluorescence was measured with a 545 nm dichroic long-pass filter and a 530/40 nm band-pass filter. Propidium iodide was measured with a 613/20 nm band-pass filter. Fluorescence histograms were gated on forward angle light scattering to exclude debris and clumped cells. For γ-H2AX, the protein level was measured by the mean value of fluorescence of the γ-H2AX histogram.

**Cytotoxicity and mutation fraction assays.** We used standard procedures to determine the surviving and mutation fractions at the TK and HPRT loci (25, 26). Briefly, cells were pretreated with CHAT (deoxycytidine, hypoxanthine, aminopterin and thymidine) for 2 days to reduce TK$^{-/-}$ and HPRT$^-$ backgrounds, then allowed to recover in THC (deoxycytidine, hypoxanthine, and thymidine) for 1 day. For surviving fractions, cells were plated immediately after irradiation at a density of 1 to 20 cells per well in 96-well plates. Colonies were scored after 10 days of incubation. For the mutation fraction, after sufficient time was allowed for phenotypic expression of mutants (3 days for TK$^{-/-}$ and 6 days for HPRT$^-$), cells were plated in the presence of 2 μg/mL trifluorothymidine for TK$^{-/-}$ mutant selection or 0.5 μg/mL 6-thioguanine for HPRT$^-$ mutant selection. The mutants can survive in the presence of selective agents and form colonies. These colonies were scored after 20 days of incubation. Plating efficiencies were determined at the same time. Plating efficiencies were calculated according to Poisson statistics, $Po = e^{-x}$, where $x$ is the average number of colony-forming cells per well and $Po$ is the observed fraction of negative wells. The mutation fraction is the ratio of plating efficiency in the presence of selective agent to the absence of selective agent (25).

**Fluorescence *in situ* hybridization.** Following irradiation, cultures were incubated for an additional 16 hours, and colcemid (0.1 μg/mL) was added during the last 4 hours to accumulate mitotic figures that were collected as previously described (28). Prior to hybridization, microscope slides were aged (2-4 days at room temperature and 2-4 hours at 37°C), treated with RNase A (100 μg/mL, 10 minutes at 37°C), fixed in 1% formaldehyde (10 minutes at room temperature), denatured in 70% formamide at 70°C for 2 minutes, and dehydrated in a cold ethanol series. A hybridization mixture containing 70% formamide and 0.1 μg/mL Cy-3-conjugated (TTAGGG)$_3$ telomeric peptide nucleic acid probe (Applied Biosystems, Foster City, CA) was hybridized to slides for 3 hours at room temperature. Slides were washed in 70% formamide (15 minutes at 30°C) and in PN (phosphate non-idet P40) buffer (0.1 mol/L Na$_2$HPO$_4$, 0.1 mol/L NaH$_2$PO$_4$, 0.1% Triton X-100) for 5 minutes at room temperature. Antifade solution containing 1.5 μg/mL of 4′,6-diamidino-2-phenylindole (Vector Laboratories Inc., Burlingame, CA) as a counterstain was applied, and the slides were coverslipped for analysis.

Our scoring criteria requires that to be scored as a telomere association, telomeres of adjacent chromosomes must be touching or very close to one another (i.e., ≤1/4 width of a chromatid) yet remain as separate and distinct signals. Twenty-five to fifty metaphases per condition were analyzed on an Olympus Provis AX-70 microscope equipped for epifluorescence. Digital images of human chromosomes were captured using a SensSys A2S black and white CCD video camera (Photometrics, Huntington Beach, CA), controlled by an Apple G3 computer, running MacProbe analysis software (Applied Imaging Corp., San Jose, CA).

## Results

**Small interfering RNA-mediated down-regulation of NBS1 protein expression in TK6 and WTK1 lines.** siRNA transfection led to a marked silencing effect of NBS1 protein expression on days 4 and 5 after transfection. We used a two-time tandem transfection approach at an interval of 1 day and cells were harvested on the 5th day after the first transfection. This protocol produced marked reduction of NBS1 protein expression (Fig. 1*A* and *B*). In cells transfected with NBS1 siRNA, the relative amount of NBS1 protein
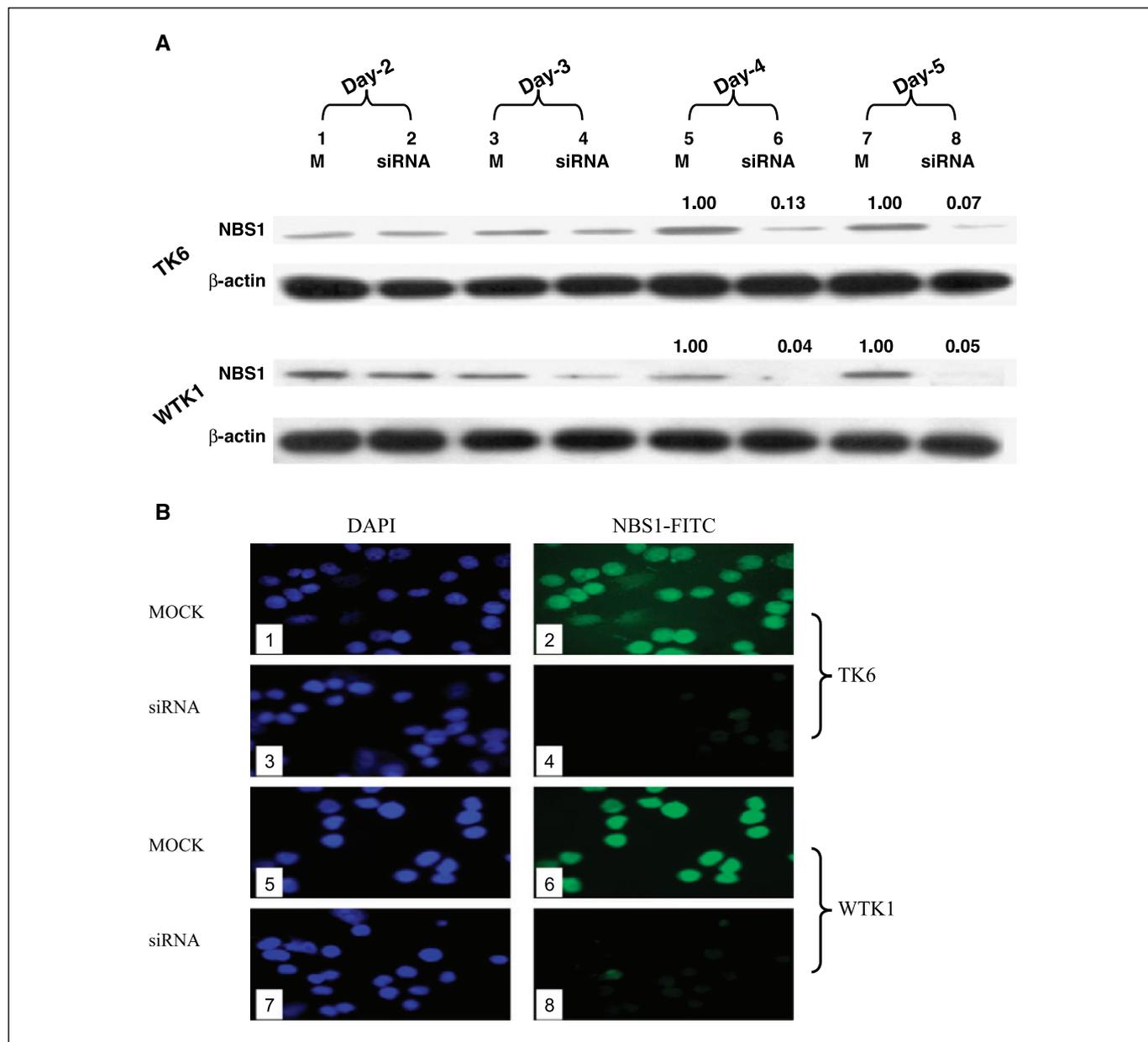


**Figure 1.** siRNA-mediated down-regulation of NBS1 protein in TK6 and WTK1 cells. Cells were harvested 2, 3, 4, and 5 days after the initial siRNA transfection to determine the level of NBS1 protein. *A,* Western blots, β-actin was included as a loading control. Numbers above bands 6 and 8 are relative levels of NBS1 as a ratio to the mock-transfected cells (bands 5 and 7) of the same day. *B,* fluorescence microscope images of cells at day 5 after siRNA transfection. Slides were stained with DAPI, probed with anti-NBS1 antibody, and a secondary FITC-conjugated antibody. 1, 2, 5, and 6 are mock-transfected cells; 3, 4, 7, and 8 are siRNA-transfected cells; 1, 2, 3, and 4 are of TK6 cells; 5, 6, 7, and 8 are of WTK1 cells; 1, 3 5, and 7 are the slides under DAPI filter to identify nuclei; 2, 4, 6, and 8 are the same fields under FITC filter to identify nuclei containing detectable NBS1 protein. Of 167 mock-transfected TK6 cells scored in six fields, strong NBS1 signals appeared in 88% of the cells, weaker signals in 8%, and no detectable signals in 4%. Of 206 NBS1 siRNA-transfected TK6 cells scored in eight fields, strong NBS1 signals appeared in 2% of the cells, weaker signals in 13%, and no detectable signals in 85%. Of 117 mock-transfected WTK1 cells scored in six fields, strong NBS1 signals appeared in 91% of the cells, weaker signals in 6%, and no detectable signals in 3%. Of 138 NBS1 siRNA-transfected WTK1 cells scored in seven fields, strong NBS1 signals appeared in 3% of the cells, weaker signals in 6%, and no detectable signals in 91%.

in TK6 cells at 4 and 5 days after introduction of siRNA was ~ 13% and 7%, respectively, of that in mock-transfected controls. The values at days 4 and 5 for WTK1 were ~ 4% and 5%. Thus, siRNA was slightly more effective at reducing NBS1 levels in WTK1 than

in TK6 (Fig. 1*A*). Consistent with the Western blot, NBS1 immunofluorescence signals were barely detectable in siRNA-transfected cells (Fig. 1*B*, 4 and 8). The results in Fig. 1, therefore, show effective silencing by the NBS1 siRNA transfection.



**Figure 2.** Downstream effects of the NBS1 knockdown. TK6 and WTK1 cells received 1.5 Gy at 5 days after the initial siRNA transfection. Numbers above bands are the relative expressional levels of proteins at indicated time points as a ratio to unirradiated control (0 hours). *A,* TK6 and WTK1 cells were harvested at the indicated times after ionizing radiation. Phospho-Chk2 (Thr$^{68}$) expression was determined by Western blot with an antibody specific for phosphorylated protein. *B,* TK6 cells were harvested at the indicated times after ionizing radiation to determine the levels of activated p53 and p21. *C,* TK6 and WTK1 cells were harvested at 24 hours after ionizing radiation. Apoptosis was measured by the ratio of sub-G$_1$ population to the total cells scored. At least 25,000 cells were scored for each sample. Each point is the average of three different experiments. *Bars*, SD.
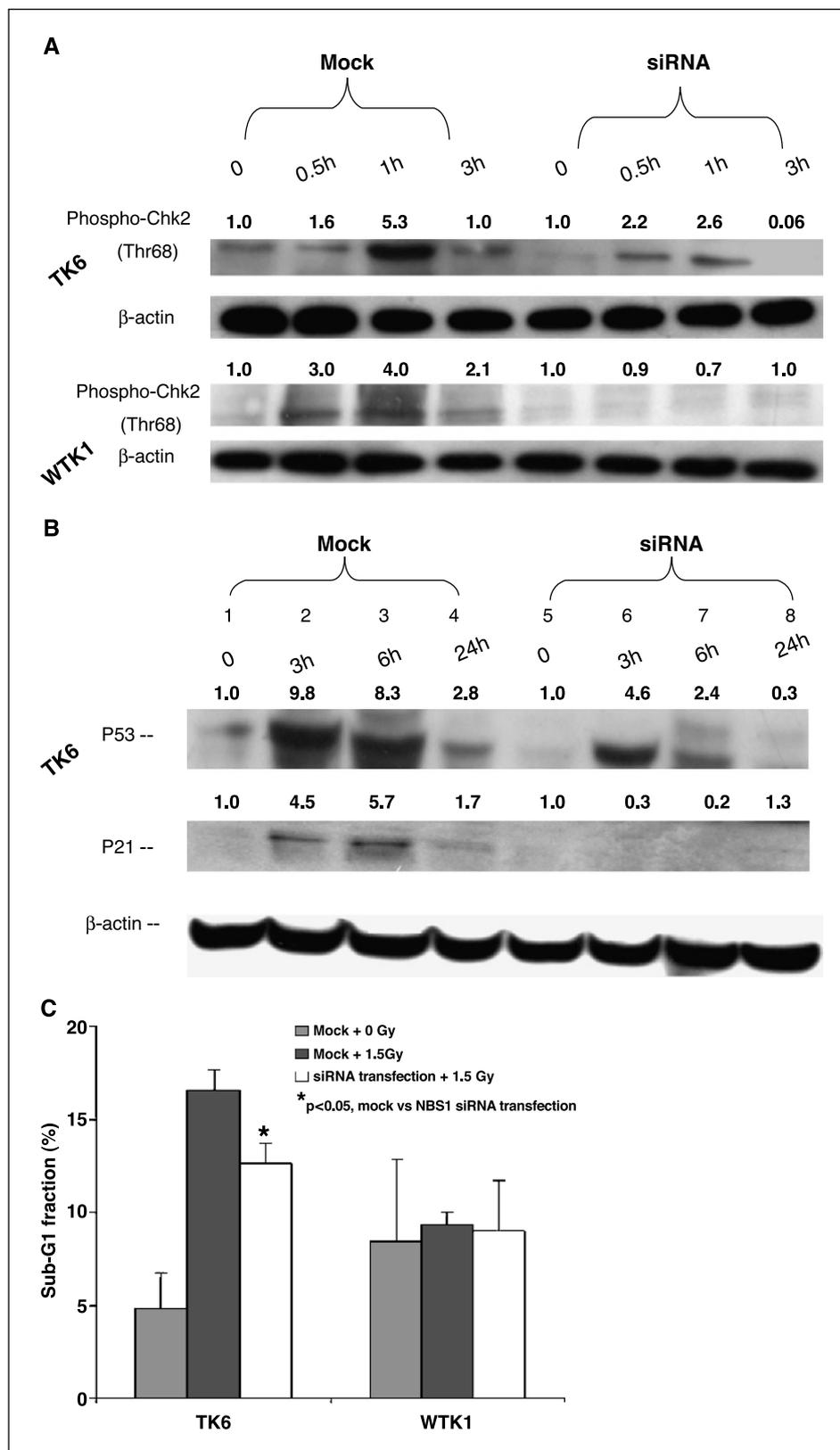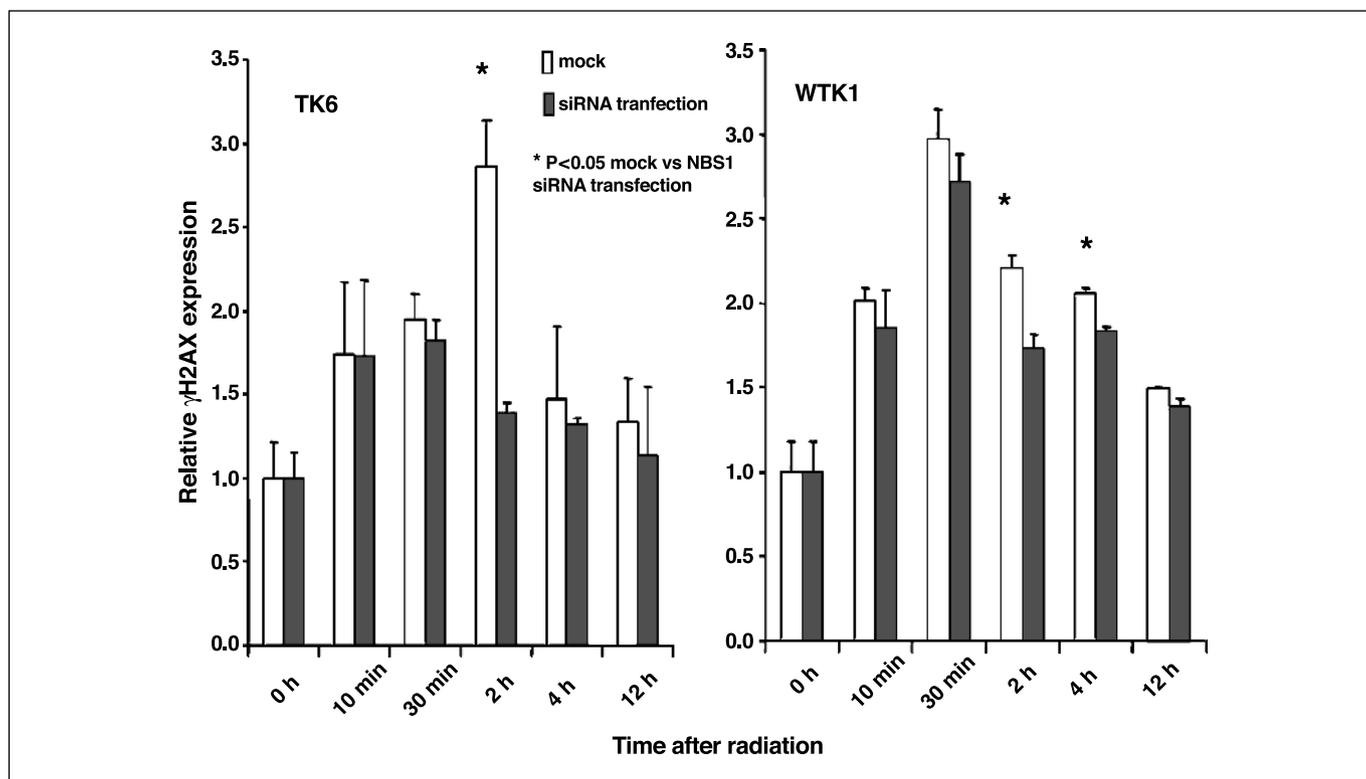
**Figure 3.** Expression of $\gamma$-H2AX as a function of time after ionizing radiation. TK6 and WTK1 cells were irradiated with 1.5 Gy 5 days after the initial siRNA transfection and harvested at different times to determine the kinetics of $\gamma$-H2AX levels. The relative level of $\gamma$-H2AX was defined as the ratio of the mean detectable $\gamma$-H2AX fluorescence signal in the entire histogram to that of unirradiated control. *Columns*, means; *bars*, SD.

**NBS1 knockdown leads to reduced Chk2 and p53 activation, as well as reduced apoptosis, after ionizing radiation.** TK6 is wild-type for p53, and WTK1 expresses only a mutated form (methionine to isoleucine substitution at codon 237; ref. 26). Compared with TK6, WTK1 cells exhibit significantly elevated background and ionizing radiation–induced mutation frequencies at the TK locus, decreased sensitivity to ionizing radiation–induced cell killing, and reduced levels of ionizing radiation–induced apoptosis (29). These two cell lines have been separate for many years, and therefore may have other differences besides p53. Both Chk2 and p53 are considered to be downstream substrates of MRN, through ATM, and to be involved in $G_1$-S, intra-S, and $G_2$-M checkpoint arrest and apoptosis (30, 31). Chk2, the mammalian homologue of *Saccharomyces cerevisiae* Rad53 and *Schizosaccharomyces pombe* Cds1, is a kinase whose activation by DNA damage prevents entry into mitosis and into S phase (32). Chk2 is activated by phosphorylation in an ATM and NBS1-dependent manner on Thr[68] after exposure to ionizing radiation. After DNA damage, Chk2

**Table 1.** Ionizing radiation–induced cell killing

| Cell line | Treatment | 0 Gy | | 0.75 Gy | | 1.5 Gy | | 3.0 Gy | |
|---|---|---|---|---|---|---|---|---|---|
| | | Number of colonies per plate | Plating efficiency (%) | Number of colonies per plate* | Surviving fraction (%)[†] | Number of colonies per plate | Surviving fraction (%) | Number of colonies per plate | Surviving fraction (%) |
| TK6 | mock | 40.7 ± 16.5 | 65.3 ± 9.2 | 27.2 ± 5.8 | 25.4 ± 4.1 | 20.5 ± 4.6 | 8.2 ± 2.0 | 15.9 ± 3.4 | 1.4 ± 0.1 |
| | siRNA | 51.8 ± 5.9 | 76.1 ± 11.2 | 35.5 ± 6.7 | 30.3 ± 5.2 | 44.2 ± 8.1 | 16.3 ± 5.2 | 28.8 ± 10.3 | 2.4 ± 0.4 |
| WTK1 | mock | 44.1 ± 7.1 | 73.8 ± 14.0 | 50.8 ± 6.6 | 58.9 ± 9.1 | 56.4 ± 8.3 | 28.3 ± 6.1 | 63.2 ± 7.8 | 9.2 ± 2.0 |
| | siRNA | 51.3 ± 6.2 | 77.3 ± 7.2 | 36.3 ± 5.4 | 31.3 ± 4.1 | 30.0 ± 6.7 | 9.3 ± 4.0 | 36.2 ± 5.3 | 3.2 ± 0.4 |

NOTE: TK6 and WTK1 cells were seeded into 96-well plates immediately after $\gamma$-irradiation. Surviving colonies were scored after 14 days of incubation. For both TK6 and WTK1 cells, 1, or 2, or 5, or 20 cells were seeded per well for 0, 0.75, 1.5, and 3 Gy, respectively. Each point is the mean and SD (three experiments done in duplicate).
*Number of colonies scored per 96-well plate.
†Surviving fraction is calculated as a ratio of plating efficiencies (the surviving fractions at 0 Gy are considered 100%).

phosphorylates p53 on Ser[20], attenuating the binding of p53 to Mdm2, a protein that targets p53 for degradation, and allowing accumulation of p53 and subsequent up-regulation of p21 (33). Up-regulation of p21 protein levels can occur transcriptionally in a p53-dependent manner, which leads to cell cycle arrest. Cell cycle arrest may provide time for cells with DNA damage to repair and decrease the chance of mutation. Cells with DNA damage blocked by cell cycle arrest can be eliminated by apoptosis if the DNA damage is not satisfactorily repaired. Thus, impaired apoptosis induction is considered one of the mechanisms to increase the fraction of mutation by failing to eliminate cells with premutagenic damage. Five days after siRNA transfection, when the expression level of NBS1 protein was barely detectable (Fig. 1*A* and *B*), cells were treated with 1.5 Gy γ-rays and harvested at various time points to determine the activation of Chk2, p21 protein level, and the accumulation of p53 protein. Figure 2*A* shows that the activation of Chk2 was detectable at 0.5, 1, and 3 hours after ionizing radiation in mock-transfected TK6 and WTK1 cells. However, NBS1 siRNA-transfected TK6 and WTK1 cells showed a marked reduction in Chk2 activation compared with mock-transfected cells. Obvious accumulation of p53 and p21 was found at 3, 6, and 24 hours in mock TK6 cells following 1.5 Gy ionizing radiation (Fig. 2*B*). In siRNA-transfected cells, the accumulations of p53 and p21 showed an obvious reduction.

Figure 2*C* shows that in mock-transfected cells, the spontaneous apoptosis levels were 4.8 ± 1.9 for TK6 cells and 8.4 ± 3.7 for WTK1 cells (mean ± SD), In siRNA-transfected cells, the spontaneous levels of apoptosis were 4.7 ± 2.1 for TK6 and 7.93 ± 4.21 for WTK1 cells (not shown in Fig. 2*C*). The level of 1.5 Gy ionizing radiation–induced apoptosis levels were 16.9 ± 1.4 and 9.2 ± 0.4 for mock-transfected TK6 and WTK1, and 11.9 ± 1.8 and 8.9 ± 2.6 for siRNA-transfected TK6 and WTK1. No statistical differences in spontaneous apoptosis levels were found between TK6 and WTK1

(Student's *t* test, 0 Gy mock-transfected TK6 versus 0 Gy mock-transfected WTK1 *P* = 0.31). No statistical differences of spontaneous apoptosis levels were found between the mock and siRNA-transfected cells (Student's *t* test, 0 Gy mock-transfected TK6 versus 0 Gy siRNA-transfected TK6 *P* = 0.93, 0 Gy mock-transfected WTK1 versus 0 Gy NBS1 siRNA-transfected WTK1 *P* = 0.88). However, ionizing radiation–induced apoptosis was significantly reduced in TK6 cells transfected with NBS1 siRNA at 24 hours after 1.5 Gy compared with mock-transfected cells (Student's *t* test, 1.5 Gy mock-transfected versus 1.5 Gy NBS1 siRNA-transfected *P* = 0.024; Fig. 2*C*), which is consistent with the failure of ionizing radiation to induce Chk2, p53, and p21 as observed in Fig. 2*A* and *B*. WTK1 cells showed the same level of apoptosis with or without NBS1 knockdown and ionizing radiation (Student's *t* test, 0 Gy mock-transfected WTK1 versus 0 Gy NBS1 siRNA-transfected *P* = 0.88, 0 Gy mock-transfected WTK1 versus 1.5 Gy mock-transfected *P* = 0.83, 1.5 Gy mock-transfected WTK1 versus 1.5 Gy NBS1 siRNA-transfected WTK1 *P* = 0.74), consistent with their mutant p53 status.

**NBS1 small interfering RNA transfection leads to decreased levels of γ-H2AX.** The phosphorylation of the histone H2AX is considered a sensor of DNA double-strand breaks. Complete or partial deficiency of H2AX resulted in a dramatically increased onset of both lymphoma and solid tumors in mice (34, 35). In fact, when H2AX levels are reduced to 50% of wild-type levels, the resultant decrease in γ-H2AX formation after ionizing radiation is insufficient to maintain genomic stability and leads to increased levels of chromosomal aberrations, reduced growth rates, and radiation sensitivity, indicating that the γ-H2AX functions in a dosage-dependent or haploinsufficient manner (34, 35). In this study, flow cytometry was used to quantify γ-H2AX levels at 10 and 30 minutes, and at 2, 4, and 12 hours after treatment with 1.5 Gy ionizing radiation (Fig. 3). The levels of γ-H2AX both in TK6 and WTK1 cells were obviously increased at 10 minutes and
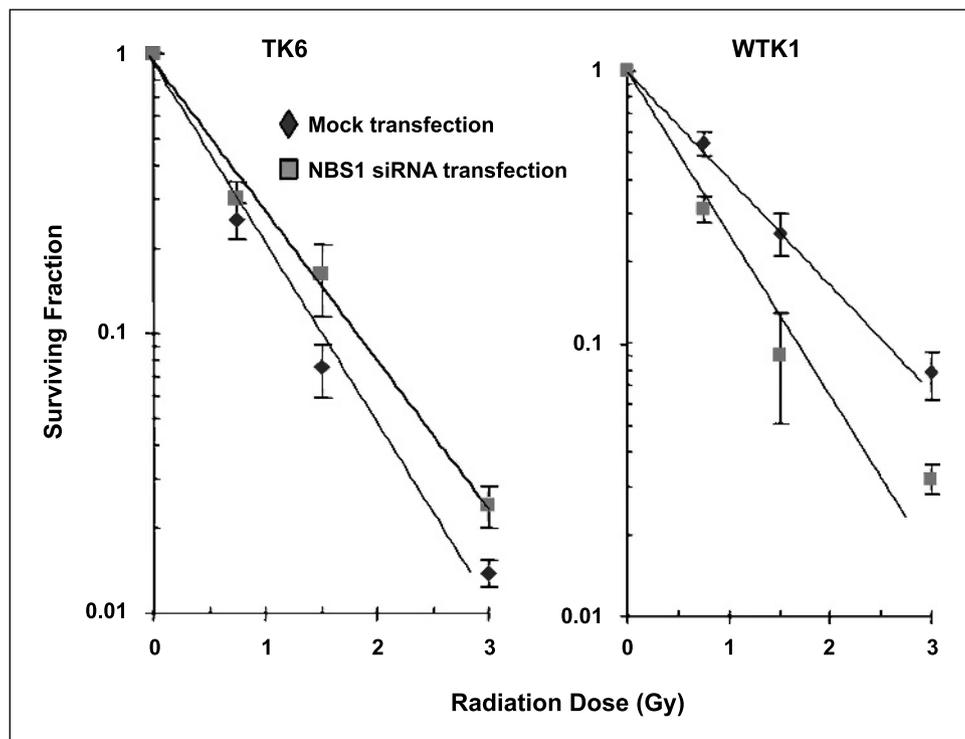


**Figure 4.** Radiation-induced cell killing in TK6 and WTK1 cells after NBS1 knockdown. On the 5th day after siRNA transfection, cells were seeded in 96-well plates, immediately after ionizing radiation. *Points*, average of three experiments; *bars*, SD. Mock transfection (♦), NBS1 siRNA transfection (■).
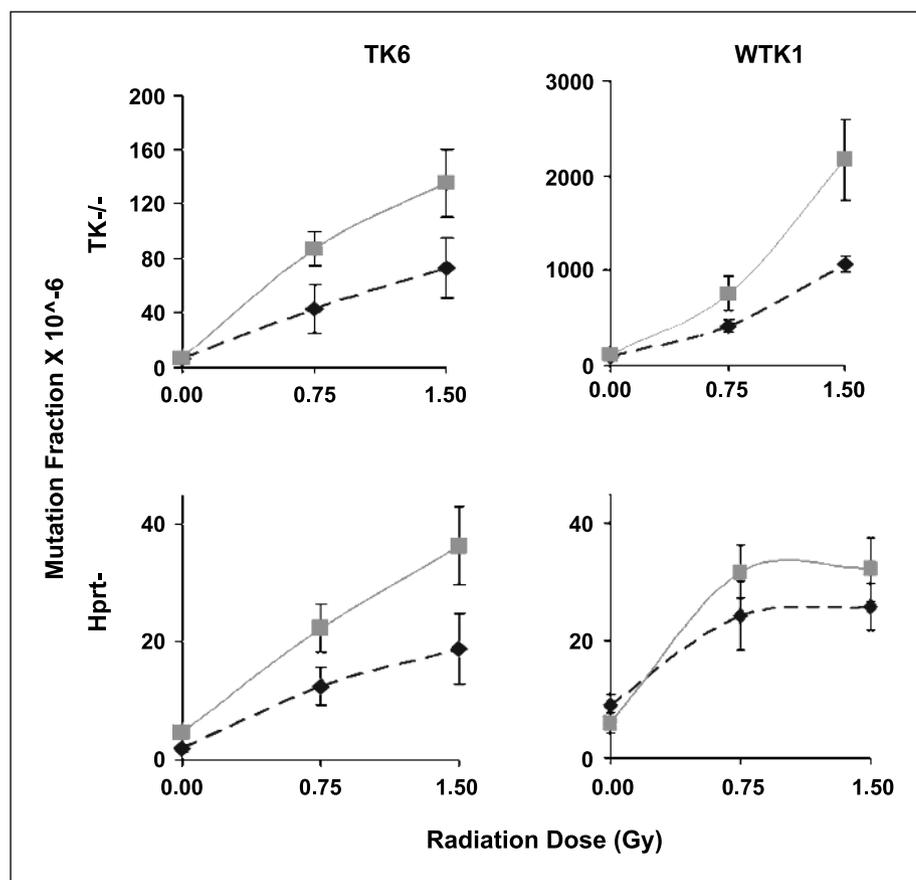
**Figure 5.** Radiation mutagenesis at the TK and HPRT loci after NBS1 knockdown. TK6 and WTK1 cells were γ-irradiated 5 days after the initial siRNA transfection. They were maintained in normal medium to allow phenotypic expression (3 days for $TK^{-/-}$ mutants and 6 days for $HPRT^-$ mutants), then were plated in the appropriate selective medium. Colonies were scored 20 days later. *Points*, average of three experiments; *bars*, SD. Note the big difference in the background and ionizing radiation–induced mutation fractions in TK6 and WTK1 cells at TK loci. Mock transfection (♦), NBS1 siRNA transfection (■).

reached maximal levels observed at 2 hours for TK6 cells and 30 minutes for WTK1 cells; the elevated levels were lower at the later time points but were still detectable even at 12 hours after ionizing radiation exposure. Both siRNA-transfected cell lines showed slightly decreased levels of γ-H2AX at the earlier time points, and significantly decreased levels at the 2-hour time point for TK6 and WTK1 cells, and at the 4-hour time point for WTK1 cells (Student's *t* test, mock-transfected versus NBS1 knockdown; $P = 0.034$ for TK6; $P = 0.014$ for WTK1 at the 2-hour time point; and $P = 0.015$ for WTK1 at the 4-hour time point).

**NBS1 knockdown renders TK6 cells less sensitive and WTK1 cells more sensitive to ionizing radiation–induced cell killing.** The radiosensitivities of mock-transfected and NBS1 siRNA-transfected TK6 and WTK1 cells were measured with a clonogenic assay (Table 1; Fig. 4). By using a regression model (36) in S-plus software, we compared the slopes of the survival curves of mock-transfected cells and NBS1 siRNA-transfected cells. The log-transformed surviving fraction showed a reasonable linear fit with the dose (Fig. 4). The slopes for mock-transfected sets are significantly different from NBS1 siRNA-transfected sets in both TK6 and WTK1—the *P* values are 0.005 for TK6 and 0.009 for WTK1. The predicted $D_0$'s (dose that reduces survival by 37% in the linear portion of the curve) for mock- and siRNA-transfected TK6 cells were 0.55 and 0.73 Gy, respectively; thus, radiosensitivity was moderately decreased by knockdown. On the other hand, knockdown increased the radiosensitivity of WTK1 cells, as the $D_0$ values for mock- and NBS1 siRNA-transfected cells were 1.14 and 0.62 Gy, respectively.

**Ionizing radiation–induced mutant fractions at the HPRT and TK Loci were increased by small interfering RNA transfection in TK6 and WTK1 cells.** Figure 5 shows mutagenesis at the HPRT and TK loci in TK6 and WTK1 cells. No quantitative differences from the knockdowns were found for background mutation fractions at either locus. After ionizing radiation, however, the knockdown produced significant increases in the mutation fraction. In TK6 cells, the mutation fractions after knockdown were about two times higher than those seen in mock-transfected cells (Student's *t* test, mock transfection versus NBS1 knockdown: for 0.75 Gy, HPRT, $P = 0.016$, TK, $P = 0.008$; for 1.5 Gy, HPRT, $P = 0.013$, TK, $P = 0.015$). In WTK1 cells, NBS1 knockdown also resulted in increased mutation fraction, although the data were significantly different only at the TK locus (Student's *t* test, mock-transfected versus NBS1 knockdown: for 0.75 Gy, HPRT, $P = 0.08$, TK, $P = 0.033$; for 1.5 Gy, HPRT, $P = 0.09$, TK, $P = 0.021$). The mutation fractions (mutants/$10^6$ cells) per $D_0$ for mock-transfected and NBS1 knockdown TK6 cells in TK locus were 34 and 89, for HPRT locus were 9 and 24, respectively. The mutation fractions per $D_0$ for mock-transfected and NBS1 knockdown WTK1 cells at the TK locus were 813 and 1,216, and at the HPRT locus were 20 and 25, respectively (Table 2).

**Induction of ionizing radiation-independent telomere association with small interfering RNA knockdown of NBS1.** The results in Table 3 show statistically significant induction of telomere instability—observed as telomere association, a phenomenon in which telomeres of the same or different chromosomes are observed in unusually close proximity in metaphase spreads—following siRNA-induced reduction of NBS1 protein levels in both

**Table 2.** Radiation mutagenesis at TK and HPRT loci after NBS1 knockdown

| Loci | Cell line | Treatment | 0 Gy | | | 0.75 Gy | | | 1.5 Gy | | |
|------|-----------|-----------|------|------|------|---------|------|------|--------|------|------|
| | | | Plating efficiency (%) | Number of colonies per plate* | Mutation fraction[†] | Plating efficiency (%) | Number of colonies per plate | Mutation fraction | Plating efficiency (%) | Number of colonies per plate | Mutation fraction |
| TK | TK6 | mock | $43.3 \pm 5.5$ | $4.8 \pm 1.5$ | $6.0 \pm 1.78$ | $45.3 \pm 4.5$ | $30.2 \pm 10.7$ | $42.7 \pm 17.8$ | $32.0 \pm 7.2$ | $34.5 \pm 5.2$ | $72.9 \pm 22.0$ |
| | | siRNA | $53.0 \pm 13.1$ | $7.5 \pm 8.5$ | $6.9 \pm 1.32$ | $43.0 \pm 1.7$ | $50.3 \pm 8.5$ | $87.0 \pm 12.6$ | $28.7 \pm 7.6$ | $50.5 \pm 5.8$ | $135.6 \pm 24.7$ |
| | WTK1 | mock | $33.3 \pm 6.8$ | $5.3 \pm 2.0$ | $87.1 \pm 16.6$ | $41.3 \pm 2.5$ | $27.2 \pm 6.4$ | $405.3 \pm 66.8$ | $30.3 \pm 2.9$ | $45.7 \pm 3.8$ | $1,065.6 \pm 80.0$ |
| | | siRNA | $35.7 \pm 7.5$ | $7.5 \pm 3.5$ | $111.5 \pm 27.7$ | $38.7 \pm 11.5$ | $40.7 \pm 7.0$ | $752.3 \pm 183.1$ | $16.7 \pm 3.1$ | $49.2 \pm 10.5$ | $2,168.4 \pm 425.8$ |
| HPRT | TK6 | mock | $62.7 \pm 11.1$ | $2.2 \pm 1.2$ | $1.9 \pm 0.7$ | $36.0 \pm 3.6$ | $8.2 \pm 1.5$ | $12.5 \pm 3.1$ | $43.3 \pm 4.0$ | $14.3 \pm 3.4$ | $18.8 \pm 6.0$ |
| | | siRNA | $58.7 \pm 10.8$ | $5.2 \pm 2.9$ | $4.7 \pm 0.6$ | $46.7 \pm 6.5$ | $17.8 \pm 3.8$ | $22.3 \pm 4.0$ | $43.7 \pm 14.6$ | $25.5 \pm 6.3$ | $36.2 \pm 6.5$ |
| | WTK1 | mock | $38.3 \pm 2.3$ | $6.3 \pm 2.3$ | $8.9 \pm 1.7$ | $36.3 \pm 1.2$ | $15.7 \pm 6.7$ | $24.3 \pm 4.4$ | $36.3 \pm 5.1$ | $16.2 \pm 3.7$ | $25.7 \pm 5.4$ |
| | | siRNA | $31.0 \pm 7.9$ | $3.5 \pm 2.4$ | $6.5 \pm 2.0$ | $42.3 \pm 2.5$ | $22.5 \pm 4.3$ | $31.7 \pm 5.8$ | $30.7 \pm 2.9$ | $17.2 \pm 2.6$ | $32.2 \pm 3.9$ |

NOTE: TK6 and WTK1 cells were treated as described in Materials and Methods and plated 3 or 7 days later to determine the mutation fraction. For TK6 cells, 20,000 cells were seeded in each well of a 96-well plate, whereas WTK1 cells were seeded at 2,000 for TK or 20,000 for HPRT. Each point is the mean and SD (three experiments done in duplicate).
*Number of mutant colonies scored in each 96-well plate. For $TK^{-/-}$, colonies are TFT-resistant, for HPRT−, colonies are 6-TG-resistant.
[†]Mutation fractions were calculated according to the description in Materials and Methods and was shown in mutants/$10^6$ cells.

## Discussion

TK6 and WTK1 cells. The ~3.3- to 4-fold increase in telomere association was independent of p53 status and did not increase after ionizing radiation exposure, supporting the view that the role of NBS1 at the telomere is distinct from its role in radiosensitivity or checkpoint control (16). These knockdown results are in agreement with our earlier analyses of human fibroblasts from Nijmegen breakage syndrome patients, where a significant increase in telomere association was also observed.[3] Here, we observed telomere association between chromatids of different chromosomes, but also noted a high incidence of telomere association between sister chromatids (Fig. 6).

### Discussion

In this study, we used siRNA transfection to transiently and selectively decrease the level of the NBS1 protein, then investigated relevant phenotypic consequences including ionizing radiation–induced mutagenesis and telomere instability. We observed that ionizing radiation–induced mutation fraction, both at the TK and HPRT loci, was increased in cells knocked down for NBS1. It seems likely that this was due to an effect on double-strand break repair. In mammalian cells, NBS1 is thought to function primarily in homologous recombination. It is important to recognize that the increase in mutations could result either from the operation of an impaired repair system that uses NBS1 or through of the use of an alternative repair system that is relatively hypermutable. In either case, the damage was repaired in some manner, as the cells containing the mutation survived. Therefore, whatever repair pathway was used must be more error-prone than the pathway that was compromised by NBS1 knockdown.

NBS1 could be involved in mutagenesis in the following way. The initial steps in the repair of double-strand breaks by homologous recombination using the sister chromatid involve the processing of DNA ends to produce 3′ single-stranded overhangs, which serve as substrates for homologous pairing and strand invasion (4). The

MRN complex is an attractive candidate complex that could provide the nuclease activity necessary to produce these tails. NBS1 is reportedly a regulator of some of the biochemical activities of the MRN complex, such as ATP-driven DNA unwinding and nuclease activity, which is necessary to process broken DNA ends (5). Repair by homologous recombination with the sister chromatid should be faithful, and mutations arising by this process should be rare. If NBS1 knockdown compromises the homologous recombination system, then errors might be more likely; alternatively, resulting use of nonhomologous end-joining could be responsible for the increased mutagenesis.

It has been shown that H2AX is mainly phosphorylated by ATM after ionizing radiation and DNA-PK acts as a supplemental kinase for this phosphorylation (5). ATM/RAD3-related is responsible for

**Table 3.** Telomere associations after NBS1 knockdown

| Cell line treatment | | Dose (Gy) | Cell scored | Telomere association | Telomere association per cell |
|---------------------|------|-----------|-------------|----------------------|-------------------------------|
| TK6 | mock | 0 | 50 | 40 | 0.8 |
| | siRNA | | 25 | 80 | 3.2 |
| | mock | 0.75 | 25 | 19 | 0.76 |
| | siRNA | | 56 | 167 | 2.98 |
| WTK1 | mock | 0 | 25 | 12 | 0.48 |
| | siRNA | | 30 | 58 | 1.93 |
| | mock | 0.75 | 25 | 15 | 0.6 |
| | siRNA | | 36 | 80 | 2.22 |

NOTE: Cells were irradiated 5 days after siRNA transfection. Chromosome slides were prepared 1 day later. Scoring was carried out double-blinded. The changes seen between mock-transfected and NBS1 knockdown cells are all statistically significant at $P < 0.01$ ($\chi^2$ analysis compares mock versus NBS1 knockdown by siRNA transfection).

---

[3] S.M. Bailey, E.H. Goodwin, and M.Z. Zdzienicka, unpublished data.
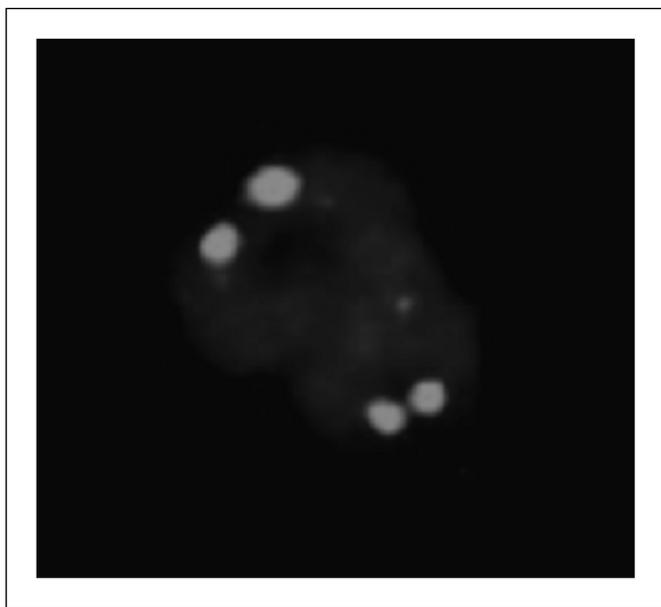
**Figure 6.** Telomere association with NBS1 knockdown. Telomere instability in an NBS1-deficient TK6 mitotic chromosome is seen as telomere association (close or touching, but still distinct telomeres) between chromatids of sisters or of different chromosomes (data not shown).

H2AX phosphorylation in S phase (37, 38). Recently published results from a number of different laboratories have shown that the MRN complex can regulate the activation of ATM and may serve as a modulator upstream of ATM (17, 18, 39). Our demonstration of reduced γ-H2AX fluorescence with NBS1 knockdown is consistent with this view. Additionally, we show that phosphorylation of the downstream ATM substrates Chk2, p53, and p21 after ionizing radiation are also decreased following NBS1 knockdown. Therefore, a second possibility to explain the increased mutation fraction is related to the decreased levels of ionizing radiation–induced γ-H2AX after NBS1 knockdown. As mentioned, the phosphorylation of H2AX modifies chromatin to allow access by repair factors for rejoining of DNA double-strand breaks; thus, the decreased phosphorylation of H2AX may impair the repair process, perhaps leading to an increase in mutation fraction.

After NBS1 knockdown, TK6 cells with a wild-type p53 showed a decreased sensitivity to ionizing radiation–induced killing, whereas WTK1 cells with a mutant p53 showed an increased sensitivity (Table 1, Fig. 4). The former result seems to be inconsistent with the well-accepted conclusion that cells derived from Nijmegen breakage syndrome patients are extremely radiosensitive (1, 2, 4, 5, 19, 40). One possible explanation for the different effects of the NBS1 knockdown on radiosensitivity in TK6 and WTK1 cells would be the following. If apoptosis mediated by p53 is responsible for much of the radiation–induced killing, its reduction would result in increased survival. On the other hand, failure to properly repair double-strand breaks would result in more cell killing. Thus, in TK6, there could be factors working in both directions and if the effect on apoptosis to increase resistance is greater than the effect

on repair to increase sensitivity, then the overall effect would be less cell killing. In WTK1, there is only the effect on repair, thus resulting in more cell killing. One fact that needs to be mentioned here is that NBS1 siRNA transfection only introduces a transient knockdown of NBS1 protein, which is different from the situation in patients with Nijmegen breakage syndrome; long-term genomic instability as a consequence of NBS1 deficiency, but not NBS1 mutation per se, may be responsible for the hyperradiosensitivity of patients Nijmegen breakage syndrome.

The increase in telomere association we observed with NBS1 knockdown was independent of radiation exposure and p53 status, supporting the view that the role of NBS1 at the telomere is distinct from its role in radiosensitivity or S phase checkpoint control (16). The observation that NBS1 associates with telomeres specifically in S phase (11) has led to the suggestion that the MRN complex is involved in either generation of the 3′ single-stranded tail, or establishment of the end-capping t-loop structure—critical features at newly replicated telomeric ends (11, 41). Additionally, activation of NBS1 by ATM is required for MRN function (14, 15, 42). It is noteworthy that not only are ataxia telangiectasia and Nijmegen breakage syndrome very similar syndromes phenotypically, but elevated occurrence of telomere association has also been reported in ataxia telangiectasia cell lines and tissues deficient in ATM (21, 22). We can speculate that if NBS1 normally functions to suppress interchromosomal recombination (5, 43), then telomere associations observed here with knockdown of NBS1 in human cells, may represent attempts at such recombination events within the repetitive telomeric tracts—not only between chromosomes, but also between sister chromatids.

Telomere shortening has been reported in cells from NBS1 patients (13) and in a cell line expressing mutant NBS1 (16). Although we did not directly measure telomere length in this study, both the transient and partial nature of the knockdown, as well as the lack of obvious diminution or absence of fluorescence *in situ* hybridization telomere signals makes it improbable that significant telomere shortening was occurring. Furthermore, both cell lines used in this study possess telomerase activity, and it has been shown that coexpression of hTERT (catalytic subunit of telomerase) and NBS1 rescues the telomere length defect seen in Nijmegen breakage syndrome cells (13).

In summary, we have shown that telomere associations and radiation–induced gene mutation are increased by NBS1 knockdown in human cells. Our demonstration of increased frequencies of such relevant phenotypes and genetic changes in human cells contributes to the understanding of possible mechanisms underlying the cancer predisposition associated with this disease.

## Acknowledgments

## References

1. Taylor AM. Chromosome instability syndromes. Best Pract Res Clin Haematol 2001;14:631–44.

2. Weemaes CM, Smeets DF, van der Burgt CJ. Nijmegen breakage syndrome: a progress report. Int J Radiat Biol 1994;66:S185–8.

3. Wilda M, Demuth I, Concannon P, Sperling K, Hameister H. Expression pattern of the Nijmegen breakage syndrome gene, Nbs1, during murine development. Hum Mol Genet 2000;9:1739–44.

4. Tauchi H, Kobayashi J, Morishima K, et al. Nbs1 is

essential for DNA repair by homologous recombination in higher vertebrate cells. Nature 2002;420:93–8.

5. Tauchi H, Matsuura S, Kobayashi J, Sakamoto S, Komatsu K. Nijmegen breakage syndrome gene, NBS1, and molecular links to factors for genome stability. Oncogene 2002;21:8967–80.

6. Buscemi G, Savio C, Zannini L, et al. Chk2 activation dependence on Nbs1 after DNA damage. Mol Cell Biol 2001;21:5214–22.

7. Siwicki JK, Degerman S, Chrzanowska KH, Roos G. Telomere maintenance and cell cycle regulation in spontaneously immortalized T-cell lines from Nijmegen breakage syndrome patients. Exp Cell Res 2003;287: 178–89.

8. Saar K, Chrzanowska KH, Stumm M, et al. The gene for the ataxia-telangiectasia variant, Nijmegen breakage syndrome, maps to a 1-cM interval on chromosome 8q21. Am J Hum Genet 1997;60:605–10.

9. Kobayashi J, Tauchi H, Sakamoto S, et al. NBS1 localizes to γ-H2AX foci through interaction with the FHA/BRCT domain. Curr Biol 2002;12:1846–51.

10. Desai-Mehta A, Cerosaletti KM, Concannon P. Distinct functional domains of nibrin mediate Mre11 binding, focus formation, and nuclear localization. Mol Cell Biol 2001;21:2184–91.

11. Zhu XD, Kuster B, Mann M, Petrini JH, de Lange T. Cell-cycle-regulated association of RAD50/MRE11/NBS1 with TRF2 and human telomeres. Nat Genet 2000;25: 347–52.

12. Eller MS, Li GZ, Firoozabadi R, Puri N, Gilchrest BA. Induction of a p95/Nbs1-mediated S phase checkpoint by telomere 3′ overhang specific DNA. FASEB J 2003;17: 152–62.

13. Ranganathan V, Heine WF, Ciccone DN, et al. Rescue of a telomere length defect of Nijmegen breakage syndrome cells requires NBS and telomerase catalytic subunit. Curr Biol 2001;11:962–6.

14. Lim DS, Kim ST, Xu B, et al. ATM phosphorylates p95/nbs1 in an S-phase checkpoint pathway. Nature 2000;404:613–7.

15. Zhao S, Weng YC, Yuan SS, et al. Functional link between ataxia-telangiectasia and Nijmegen breakage syndrome gene products. Nature 2000;405:473–7.

16. Bai Y, Murnane JP. Telomere instability in a human tumor cell line expressing NBS1 with mutations at sites phosphorylated by ATM. Mol Cancer Res 2003;1: 1058–69.

17. Carson CT, Schwartz RA, Stracker TH, Lilley CE, Lee DV, Weitzman MD. The Mre11 complex is required for ATM activation and the $G_2/M$ checkpoint. EMBO J 2003;22:6610–20.

18. Uziel T, Lerenthal Y, Moyal L, Andegeko Y, Mittelman L, Shiloh Y. Requirement of the MRN complex for ATM activation by DNA damage. EMBO J 2003;22:5612–21.

19. van der Burgt I, Chrzanowska KH, Smeets D, Weemaes C. Nijmegen breakage syndrome. J Med Genet 1996;33:153–6.

20. Dumon-Jones V, Frappart PO, Tong WM, et al. Nbn heterozygosity renders mice susceptible to tumor formation and ionizing radiation-induced tumorigenesis. Cancer Res 2003;63:7263–9.

21. Kojis TL, Gatti RA, Sparkes RS. The cytogenetics of ataxia telangiectasia. Cancer Genet Cytogenet 1991;56: 143–56.

22. Pandita TK, Pathak S, Geard CR. Chromosome end associations, telomeres and telomerase activity in ataxia telangiectasia cells. Cytogenet Cell Genet 1995;71:86–93.

23. Paz-y-Mino C, Sanchez ME, Del Pozo M, et al. Telomeric association in women with breast and uterine cervix cancer. Cancer Genet Cytogenet 1997;98:115–8.

24. Bedford JS, Liber HL. Applications of RNA interference for studies in DNA damage processing, genome stability, mutagenesis, and cancer. Semin Cancer Biol 2003;13:301–8.

25. Liber HL, Thilly WG. Mutation assay at the thymidine kinase locus in diploid human lymphoblasts. Mutat Res 1982;94:467–85.

26. Xia F, Wang X, Wang YH, et al. Altered p53 status correlates with differences in sensitivity to radiation-induced mutation and apoptosis in two closely related human lymphoblast lines. Cancer Res 1995;55:12–5.

27. Gong J, Traganos F, Darzynkiewicz Z. A selective procedure for DNA extraction from apoptotic cells applicable for gel electrophoresis and flow cytometry. Anal Biochem 1994;218:314–9.

28. Bailey SM, Meyne J, Chen DJ, et al. DNA double-strand break repair proteins are required to cap the ends of mammalian chromosomes. Proc Natl Acad Sci U S A 1999;96:14899–904.

29. Xia F, Liber HL. The tumor suppressor p53 modifies mutational processes in a human lymphoblastoid cell line. Mutat Res 1997;373:87–97.

30. Jack MT, Woo RA, Motoyama N, Takai H, Lee PW. DNA-dependent protein kinase and checkpoint kinase 2 synergistically activate a latent population of p53 upon DNA damage. J Biol Chem 2004;279:15269–73.

31. Hirao A, Kong YY, Matsuoka S, et al. DNA damage-induced activation of p53 by the checkpoint kinase Chk2. Science 2000;287:1824–7.

32. Matsuoka S, Huang M, Elledge SJ. Linkage of ATM to cell cycle regulation by the Chk2 protein kinase. Science 1998;282:1893–7.

33. Hirao A, Cheung A, Duncan G, et al. Chk2 is a tumor suppressor that regulates apoptosis in both an ataxia telangiectasia mutated (ATM)-dependent and an ATM-independent manner. Mol Cell Biol 2002;22: 6521–32.

34. Celeste A, Difilippantonio S, Difilippantonio MJ, et al. H2AX haploinsufficiency modifies genomic stability and tumor susceptibility. Cell 2003;114:371–83.

35. Bassing CH, Suh H, Ferguson DO, et al. Histone H2AX: a dosage-dependent suppressor of oncogenic translocations and tumors. Cell 2003;114:359–70.

36. Neter J, Kuther MH, Wasserman W, Nachtsheim CJ. Applied linear statistical models. 4th ed. New York: McGraw-Hill;1996.

37. Yoshida K, Yoshida SH, Shimoda C, Morita T. Expression and radiation-induced phosphorylation of histone H2AX in mammalian cells. J Radiat Res (Tokyo) 2003;44:47–51.

38. Stiff T, O'Driscoll M, Rief N, Iwabuchi K, Lobrich M, Jeggo PA. ATM and DNA-PK function redundantly to phosphorylate H2AX after exposure to ionizing radiation. Cancer Res 2004;64:2390–6.

39. Horejsi Z, Falck J, Bakkenist CJ, Kastan MB, Lukas J, Bartek J. Distinct functional domains of Nbs1 modulate the timing and magnitude of ATM activation after low doses of ionizing radiation. Oncogene 2004;23: 3122–7.

40. Komatsu K, Yoshida M, Okumura Y. Murine scid cells complement ataxia-telangiectasia cells and show a normal post-irradiation response of DNA synthesis. Int J Radiat Biol 1993;63:725–30.

41. de Lange T, Petrini JH. A new connection at human telomeres: association of the Mre11 complex with TRF2. Cold Spring Harb Symp Quant Biol 2000; 65:265–73.

42. Wu X, Ranganathan V, Weisman DS, et al. ATM phosphorylation of Nijmegen breakage syndrome protein is required in a DNA damage response. Nature 2000;405:477–82.

43. Johnson RD, Jasin M. Sister chromatid gene conversion is a prominent double-strand break repair pathway in mammalian cells. EMBO J 2000;19:3398–407.

# Cancer Research

AACR American Association for Cancer Research

# *NBS1* Knockdown by Small Interfering RNA Increases Ionizing Radiation Mutagenesis and Telomere Association in Human Cells

Ying Zhang, Chang U.K. Lim, Eli S. Williams, et al.

| | |
|---|---|
| **Updated version** | Access the most recent version of this article at:<br>http://cancerres.aacrjournals.org/content/65/13/5544 |

| | |
|---|---|
| **Cited articles** | This article cites 42 articles, 16 of which you can access for free at:<br>http://cancerres.aacrjournals.org/content/65/13/5544.full#ref-list-1 |
| **Citing articles** | This article has been cited by 7 HighWire-hosted articles. Access the articles at:<br>http://cancerres.aacrjournals.org/content/65/13/5544.full#related-urls |

| | |
|---|---|
| **E-mail alerts** | Sign up to receive free email-alerts related to this article or journal. |
| **Reprints and Subscriptions** | To order reprints of this article or to subscribe to the journal, contact the AACR Publications Department at pubs@aacr.org. |
| **Permissions** | To request permission to re-use all or part of this article, use this link<br>http://cancerres.aacrjournals.org/content/65/13/5544.<br>Click on "Request Permissions" which will take you to the Copyright Clearance Center's (CCC)<br>Rightslink site. |